Kibble-Zurek scaling and its breakdown for spontaneous generation of Josephson vortices in Bose-Einstein condensates

Shih-Wei Su,[1] Shih-Chuan Gou,[2] Ashton Bradley,[3] Oleksandr Fialko,[4] and Joachim Brand[4]

[1]*Department of Physics, National Tsing Hua University, Hsinchu 30013 Taiwan*
[2]*Department of Physics and Graduate Institute of Photonics,*
National Changhua University of Education, Changhua 50058 Taiwan
[3]*Jack Dodd Centre for Quantum Technology, Department of Physics, University of Otago, Dunedin, New Zealand*
[4]*Centre for Theoretical Chemistry and Physics, New Zealand Institute for Advanced Study,*
Massey University (Albany Campus), Auckland, New Zealand
(Dated: Version of February 15, 2013.)

Atomic Bose-Einstein condensates confined to a dual-ring trap support Josephson vortices as topologically stable defects in the relative phase. We propose a test of the scaling laws for defect formation by quenching a Bose gas to degeneracy in this geometry. Stochastic Gross-Pitaevskii simulations reveal a $-1/4$ power-law scaling of defect number with quench time for fast quenches, consistent with the Kibble-Zurek mechanism. Slow quenches show stronger quench-time dependence that is explained by the stability properties of Josephson vortices, revealing the boundary of the Kibble-Zurek regime. Interference of the two atomic fields enables clear long-time measurement of stable defects, and a direct test of the Kibble-Zurek mechanism in Bose-Einstein condensation.

A possible mechanism for the formation of domain structures in the early universe was proposed by Kibble [1]. In this original paper, it was argued that the Universe cooled down after the hot Big Bang event and subsequently passed through a symmetry breaking phase transition with critical temperature T_c. Causally unconnected spatial domains settling into different vacua would lead to the formation of defects like domain walls, monopoles, strings, textures, etc [2]. Due to thermal fluctuations thwarting the emerging order, it was postulated that the number of defects eventually settled at the so-called Ginzburg temperature $T_G < T_c$.

Later Zurek [3] put forward an alternative argument that focused on the nonequilibrium aspect of the phase transition. The density of the defects is determined at the critical temperature instead and its number is scaled with the quench rate. The scaling exponent depends on the critical exponents of the underlying phase transition. This scenario, known as the Kibble-Zurek mechanism (KZM) should equally apply to condensed matter phase transitions where it is accessible to laboratory experiments [4]. The KZM proved to be robust and was verified by a number of recent experiments on superconductors [5–8] and theoretical research on Bose-Einstein condensates (BEC) [9, 11, 12, 15]. It also extends to quantum phase transitions [10, 13, 14].

In the spirit of Kibble's original argument one might expect the KZM to fail in the limit of slow quenches where the time scale of other processes occurring in the system dominates over the quench time. Deviations from KZM predictions were observed in ^{4}He experiments [16] but interpretation was controversial [17] and a manifestation of the Ginzburg temperature was ruled out in Ref. [18]. So far a transition between a regime of KZM scaling and its breakdown has not been studied systematically.
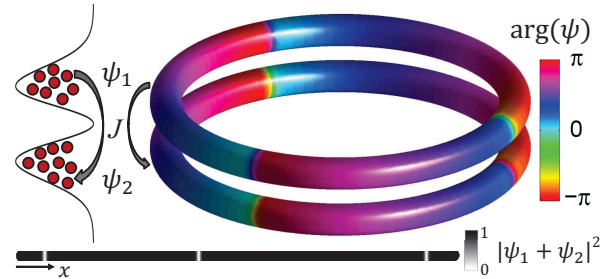

FIG. 1. (Color online) Schematic of the two linearly coupled BECs. The isosurface shows the equilibrated condensate density profile for a double-ring trap configuration and the color shows a phase profile with three Josephson vortices resulting from a quench at fixed tunneling energy J. The solid line on the left visualizes the trapping potential in the vertical direction, which forms a double well. The interference pattern of the two atomic fields on the bottom shows clear evidence of the Josephson vortices which are characterized by the low density regions.

In this Letter we investigate the robustness of the KZM in a model system where departure from KZM scaling can be understood in detail because the defects are easily quantified and are stable at the end of the quench. This avoids the difficulty of counting the decaying population of defects [11, 20] or their remnants [19]. To this end, we study two linearly coupled quasi-one-dimensional (quasi-1D) atomic Bose gases in the ring configuration, as in Fig. 1. A quench through the Bose-Einstein condensation phase transition can generate Josephson vortices (JVs) confined between the two BECs [21, 22]. We show that the number of these defects obeys the Kibble-Zurek scaling law for fast quenches. On the contrary, for slow quenches, the predicted behavior deviates substantially and we observe a much stronger quench-time dependence than expected for critical phenomena in our

simulations. This is due to decay processes occurring before topological stability is established, in analogy to Kibble's arguments.

We consider two linearly coupled Bose gas in the quasi-1D ring geometry. The trapping potential can be realized by crossing a vertical Gaussian-Laguerre laser beam (LG_0^1) and two horizontal sheet beams [24] to form an optical dipole trap or with rf-dressing on an atom chip [23]. Along the z-axis the trapping potential can be treated as a double-well potential as shown on the left of Fig. 1. Assuming tight confinement, the transverse degrees of freedom can be eliminated. The resulting coupled quasi-1D Gross-Pitaevskii equations for the BEC order parameter ψ_1 and ψ_2 in each ring assume the dimensionless form

$$i\partial_t \psi_j = (\mathcal{L}_j - \mu)\psi_j - J\psi_{3-j} \qquad (1)$$

where $\mathcal{L}_j = -\frac{1}{2}\partial_{xx} + g|\psi_j|^2$ and $j = 1, 2$. Length (x), time (t), and energy (μ, J) are given in the harmonic oscillator units of $a_h = \sqrt{\hbar/m\omega}$, $t_h = 1/\omega$, and $E_h = \hbar\omega$, respectively, where m is the atomic mass and ω is the trapping frequency in the transverse direction. Dimensionless $g = 2a/a_h$ is the non-linear interaction strength with the s-wave scattering length a; μ is the chemical potential, and J is the tunneling energy.

Equation (1) supports topological and non-topological defects in the form of the JV and the dark soliton, respectively,

$$\tilde{\psi}_{1,2} = \sqrt{1+\nu}\tanh(p\tilde{x}) \pm iB\operatorname{sech}(p\tilde{x}), \qquad (2)$$

where $\nu = J/\mu$, and the scaling $x = \sqrt{\mu}\tilde{x}$ and $\psi_j = \sqrt{\mu/g}\tilde{\psi}_j$ has been applied. Both the dark soliton with $B = 0$ and $p = \sqrt{1+\nu}$ and the JV with $p = 2\sqrt{\nu}$ and $B = \sqrt{1-3\nu}$ for $\nu \leq 1/3$ are excitations above the vacuum where $\psi_1 = \psi_2 = $ const and are localized on the length scale $a_h(\sqrt{\mu}p)^{-1}$ [21]. The dark soliton, where both components have identical profiles, is non-topological because it is continuously connected to the vacuum by a family of moving "grey" solitons with decreasing energy [25]. Although they may be present transiently during a quench through the BEC phase transition, dark solitons will thus not survive the final stage of cooling. Furthermore, for $\nu < 1/3$, dark solitons are dynamically unstable with respect to the decay into JVs, which have lower energy [26]. The stability properties of the JV, on the other hand, depend on the dimensionless parameter ν and may change during the quench. The JV bifurcates from the dark soliton at $\nu = 1/3$ as a time-reversal symmetry broken state (vortex and anti-vortex) with a characteristic phase winding of 2π around a point located between the two rings (see Fig. 1), and only exists for smaller values of ν. From numerical simulations it is known that JVs can move with respect to the background BEC, although explicit solutions are unknown. For $1/5 < \nu < 1/3$ perturbative arguments indicate that the JV is energetically unstable [26]. For $\nu < 1/5$ where

the JV resembles the Sine-Gordon soliton [21, 22], the stationary solution (2) is a metastable local energy minimum, since the energy increases with velocity. Thus, at sufficiently small ν, JVs are topologically stable, enabling experimental tests of the KZM scaling by counting the number of JVs at the end of the quench in a dual-ring BEC. The defects would be immediately evident by interference of the two atomic fields via expansion imaging. The situation is strikingly different to a single one-dimensional BEC where the KZM scaling law was predicted to govern a transient population of dark solitons that finally decays, which makes experimental detection more difficult [11].

The nonequilibrium dynamics during the thermal quenches can be described by the coupled stochastic Gross-Pitaevskii equations [27, 28]:

$$d\psi_j = (i+\Gamma)\left[(\mu(t) - \mathcal{L}_j)\psi_j + J\psi_{3-j}\right]dt + dW_j, \quad (3)$$

where Γ is the growth rate, and μ is the chemical potential of the thermal cloud. dW_j is the white noise associated with the growth process, which is characterized by the fluctuation-dissipation relation $\langle dW_j^*(x,t)\,dW_k(x',t)\rangle = 2\Gamma T\delta_{jk}\delta(x-x')\,dt$, where T is the temperature in units of $\hbar\omega/k_B$. At the mean field equilibrium level the phase transition is described by the ground state of the energy $\mathcal{H} = \int dx\,\frac{1}{2}|\partial_x\psi_1|^2 + \frac{1}{2}|\partial_x\psi_2|^2 + V(\psi_1, \psi_2)$, where we seek the minimum of the potential $V(\psi_1, \psi_2) \equiv \sum_{j=1,2}|\psi_j|^2\left[\frac{g}{2}|\psi_j|^2 - \mu\right] - J\left[\psi_1^*\psi_2 + \psi_2^*\psi_1\right]$ for $J > 0$. The symmetry $V(\psi_1, \psi_2) = V(\psi_2, \psi_1)$ imposes a common amplitude for the ground state fields. Taking $\psi_1 = \sqrt{n}e^{i\theta_1}$, $\psi_2 = \sqrt{n}e^{i\theta_2}$, and $\Delta = \theta_1 - \theta_2$, the minimum of $V = gn^2 - 2\mu n - 2Jn\cos\Delta$ occurs at $\Delta = 0$, $n = (\mu + J)/g$, for $\mu > -J$. At the critical point $\mu = -J$ the minimum is independent of Δ and each field can acquire a $U(1)$ symmetry-breaking phase.

The dynamical transition to the broken symmetry phase is simulated via Eq. (3) with time-dependent chemical potential

$$\mu(t) = t/\tau_Q, \qquad (4)$$

where τ_Q is the quench time. The quench starts from a thermal gas with chemical potential $-\mu_0 < 0$, and ceases in the Bose-condensed phase at $\mu_0 > 0$. Due to the coupling between the two rings $\tilde{\mu}(t) = t/\tau_Q + J$ acts as the effective chemical potential in mean field theory; the precise location of the transition in a dynamical quench must be determined numerically. To count the number of JVs during the quench, we evaluate the total phase defined as $\theta_i = \oint d\theta_i$ for the i-th ring. Consequently the total number of JVs can be quantified by calculating $N_{JV} = \oint |d(\theta_1 - \theta_2)|/2\pi$.

Kibble-Zurek theory applied to the BEC phase transition gives the relaxation time and healing length close to the critical point as

$$\tau = \tau_0|\tilde{\mu}|^{-1}, \quad \xi = \xi_0|\tilde{\mu}|^{-1/2}, \qquad (5)$$
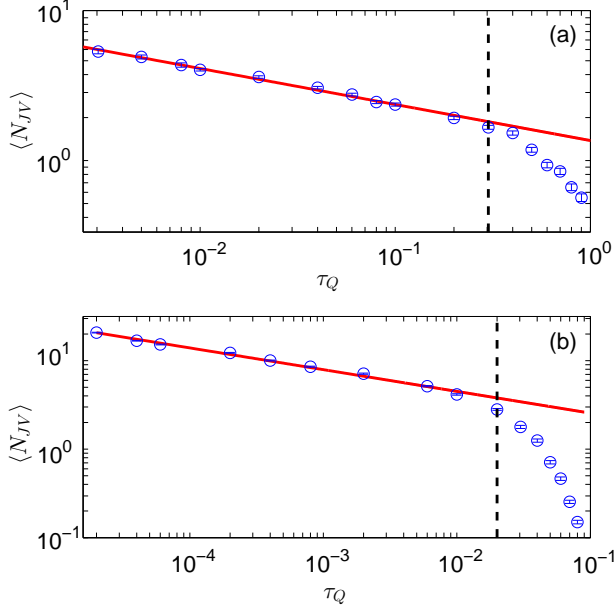
FIG. 2. (Color online) Scaling of the total number of JVs $\langle N_{JV} \rangle$ with respect to τ_Q at $J = 5$ in (a) and $J = 25$ in (b) averaged from 500 trajectories of Eq. (3). The error bars indicate the standard deviations. The red lines show the best power-law fit for fast quenches with exponents -0.2523 ± 0.0128 in (a) and -0.2456 ± 0.0131 in (b). These fit very well with the KZM prediction of -1/4. The dashed lines indicate the critical quench time τ_Q^{crit} of Eq. (10) for the breakdown of the KZM scaling law.

where ξ_0 and τ_0 depend on the microscopic details of the system. Using Eq. (4) and following the Kibble-Zurek scenario [29], we obtain the typical size of the domains after the quench

$$\hat{\xi} = \xi_0 \left(\frac{\tau_Q}{\tau_0} \right)^{1/4}, \qquad (6)$$

where for our system $\tau_0 = \Gamma^{-1}$. When $\mu(t)$ exceeds $-J$, localized phase-domains start to grow in each ring. Typically a piece of the (anti-)vortex will fall within a ξ-sized domain and the phase in each domain is chosen independently and randomly. Therefore, for small J, in a ring with circumference C, the total number of JVs is estimated to be

$$\langle N_{JV} \rangle \sim C/\hat{\xi} = C\xi_0^{-1} \left(\frac{\tau_Q}{\tau_0} \right)^{-1/4}, \qquad (7)$$

and thus obeys the $-1/4$ power-law scaling with quench time. The number of JVs thus shows a stronger quench-time dependence than the winding number of a single-ring BEC, which was predicted to scale with $\tau_Q^{-1/8}$ [15].

We consider a gas of ^{87}Rb atoms with a transverse confining frequency of $\omega = 2\pi \times 200$Hz and corresponding

nonlinear interaction strength $g = 0.05$. To study the quench dynamics we numerically integrate Eq. (3) with circumference $C = 30$ and $T = 10^{-3}$. All these parameters are realistic, e.g. with the set-up of Ref. [30]. The scaling in Eq. (7) is verified by averaging N_{JV} over 500 trajectories for two tunneling energies, $J = 5$ and 25. The quenches vary the chemical potential from $-\mu_0$ to $+\mu_0$, with μ_0 sufficiently large that the resulting defect number is independent of it. As shown in Fig. 2, the simulation results of fast quenches compare favorably with the KZM prediction, however the number of JVs deviates from the KZM scaling for slow quenches.

The stability of a JV depends on conditions that change during the quench. According to the KZM, two different regimes exist: For early as well as late times during the quench, relaxation is efficient and fluctuations in the Bose gas follow the changing chemical potential adiabatically. However, when the diverging relaxation time τ of Eq. (5) exceeds the time scale of the quench $\mu/\dot{\mu}$, fluctuations transiently freeze out and the system enters the *impulse* regime. This occurs when

$$\tau(\tilde{\mu}(\hat{t})) = |\tilde{\mu}/\dot{\tilde{\mu}}|_{t=\hat{t}} = \hat{t}, \qquad (8)$$

giving the freeze-out timescale $\hat{t} = \sqrt{\tau_0 \tau_Q}$. At the following impulse–adiabatic transition the frozen fluctuations are imprinted onto the forming BEC. We thus expect that the stability properties of formed defects at this transition point determine their survival during the adiabatic phase of the quench.

A convenient observable to detect the impulse-adiabatic transition is the particle number, which is shown in Fig. 3. While the particle number is small in the impulse regime, it follows the dashed linear time-dependence in the adiabatic regime. Figure 3 shows clear evidence of the impulse-adiabatic transition happening at $\tilde{\mu} = f\hat{t}/\tau_Q$, with a value of $f \approx 4.7$ read off the numerical data; the value of f appears to depend only weakly on the details of the system, including the parameters J and Γ, consistent with the theoretical argument that $\tilde{\mu}$ is relevant for the quench dynamics. Similar behavior was observed for a single ring BEC [15]. Therefore we can predict the chemical potential at the impulse-adiabatic transition as:

$$\hat{\mu} = \mu \left(f\hat{t} - \tau_Q J \right) = f\sqrt{\frac{\tau_0}{\tau_Q}} - J. \qquad (9)$$

We denote the critical ratio of tunneling to chemical potential for JV stability by $\nu_c = J/\mu_c$, where μ_c is the stabilizing chemical potential for given J. As shown in Fig. 4(a), the defects are frozen in until $\hat{\mu} > \mu_c$ for fast quenches ensuring the topological protection of JVs and hence the KZM signature. However, for slow quenches the impulse regime terminates earlier with $\hat{\mu} < \mu_c$, which causes the decay of the JVs in the shaded region in Fig. 4 until the topological stability of JV is established at $\mu(t) = \mu_c$. Although the the stability properties of
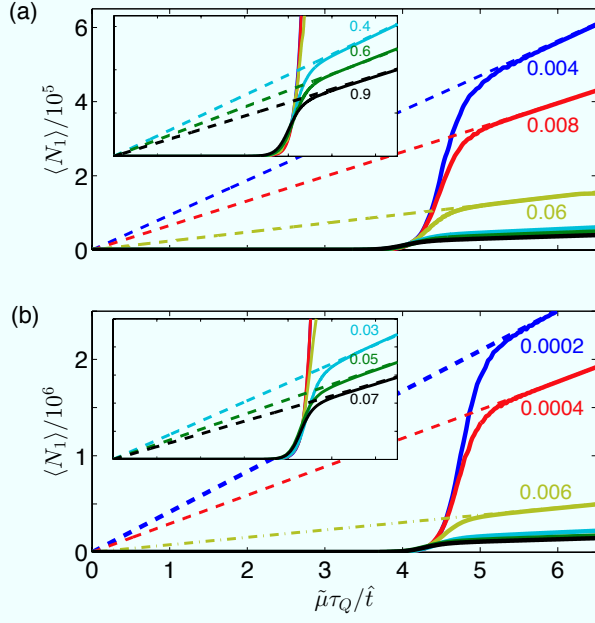
FIG. 4. (Color online) Schematic plots of the relaxation time $\tau = \tau_0/|\tilde{\mu}|$ vs. chemical potential. During the quench, the system moves from left to right along the horizontal axis. $\hat{\mu}$ is the chemical potential at the impulse-adiabatic transition and μ_c is the critical potential for stabilizing JVs, which are stable to the right of the dashed line. Panel (a) shows the fast quench where the KZM scaling is not affected by the stability of JV. Panel (b) represents a slow quench where the resulting number of defects is affected by decay processes taking place in the shaded area.

FIG. 3. (Color online) Particle number of component ψ_1 as a function of time for $J = 5$ in (a) and $J = 25$ in (b). The inset enlargements have the vertical scale magnified by a factor of 10 and reveal details for slow quenches. The color-coded labels show τ_Q. Quenches with vastly different τ_Q show a knee structure characteristic of the impulse-adiabatic transition with a rapid particle number increase around $\tilde{\mu}\tau_Q/\hat{t} = 4.7$ for both $J = 5$ and 25.

the static JV at equilibrium are known, the critical ν_c for a moving JV at finite temperatures remains unclear. Nevertheless we can estimate ν_c from the numerical simulations, as the point where the JV becomes unstable. From Eq. (9) we obtain the criterion for obtaining stable JVs

$$\tau_Q < \tau_Q^{crit} = \tau_0 f^2 (\nu_c/J)^2 (1 + \nu_c)^{-2}. \qquad (10)$$

The value $\nu_c \simeq 0.0813$ is obtained from the data for $J = 5$. With this value at hand, we can predict $\tau_Q^{crit} = 0.02$ for $J = 25$, as shown by the vertical dashed line plotted in Fig. 2(b). This prediction agrees with the numerical data very well. The critical quench time depends on the growth rate through τ_0 and we have also verified the prediction of Eq. (10) at different growth rates. In the slow quench regime the defect number varies much more strongly with quench time than expected from the KZM as is seen by the negative gradient of large magnitude seen in Fig. 2. Since the gradient is clearly much stronger than the $-1/4$ expected from the standard argument behind Eq. (7), we do not expect to enter a new regime of power-law scaling for slow quenches. It should be noted that slow quenches show the same knee structure characteristic of the impulse-adiabatic transition as the fast quenches that lead to KZ scaling (Fig. 3). We have also verified that the defect numbers for slow quenches continue to satisfy the KZM scaling (solid line in Fig. 2)
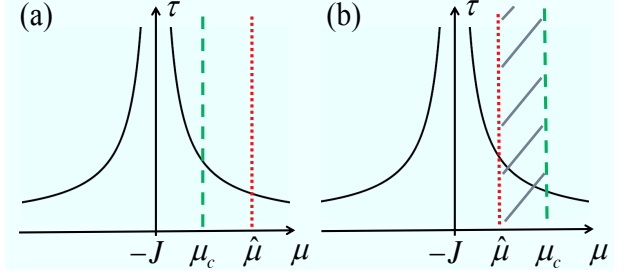
when counted immediately after the impulse-adiabatic transition at $\hat{\mu}$. This supports our argument that the reduced defect number is due to thermal decay processes happening after the transition, and that spontaneous defect formation is not affected by thermal fluctuations during freeze-out.

For JVs, the regime for slow quenches is similar to the original idea put forward by Kibble [1], where thermal fluctuations may still have enough time to destroy the emerging order before the decreasing temperature approaches the Ginzburg temperature. We observe a Ginzburg-like regime where thermal effects destroy the pattern of symmetry breaking inherited from criticality during the interval $\hat{\mu} < \mu < \mu_c$, shown in the shaded region of Fig. 4(b).

The absence of any striking, clear cut evidence of cosmological nature and the difficulty in observing the KZM in condensed-matter experiments despite its dramatic predictions is usually not attributed to the failure of the mechanism but may be explained by the eventual decay of defects in the post-quench era [11, 19, 20]. This difficulty is circumvented if the formed defects are manifestly protected from post-quench decay, e.g. by topology. The defects observed in the successful experiments of Refs. [5–8] have this property as do the JVs that are the subject of this Letter. While cosmological defects protected by topology may still survive in dark matter or dark energy, their detection is difficult [31].

Our work paves the way for a direct test of KZM in the Bose-Einstein condensation phase transition, by eliminating post-quench decay of defects. The quench of μ could be supplanted by a controlled sweep of J, providing another knob for varying the quench time.

[1] T. W. Kibble, J. Phys. A: Math. Gen. **9**, 1387 (1976).
[2] A. Vilenkin and E. P. S. Shellard, *Cosmic Strings and Other Topological Defects* (Cambridge University Press, Cambridge, UK, 1994).
[3] W. H. Zurek, Nature **317**, 505 (1983).
[4] T. Kibble, Physics Today **60**, 47 (2007).
[5] R. Monaco, J. Mygind, and R. J. Rivers, Phys. Rev. Lett. **89**, 080603 (2002).
[6] R. Monaco, J. Mygind, and R. J. Rivers, Phys. Rev. B **67**, 104506 (2003).
[7] R. Monaco, M. Aaroe, J. Mygind, R. J. Rivers, and V. P. Koshelets, Phys. Rev. B **74**, 144513 (2006).
[8] R. Monaco, J. Mygind, M. Aaroe, R. J. Rivers, and V. P. Koshelets, Phys. Rev. Lett. **96**, 180604 (2006).
[9] W. H. Zurek, Phys. Rev. Lett. **102**, 105702 (2009).
[10] J. Dziarmaga, J. Meisner, and W. J. Zurek, Phys. Rev. Lett. **101**, 115701 (2008).
[11] B. Damski and W. H. Zurek, Phys. Rev. Lett. **104**, 160404 (2010).
[12] A. del Campo, A. Retzker, and M. B. Plenio, New J. Phys. **13** 083022 (2011).
[13] J. Sabbatini, W. H. Zurek, and M. J. Davis, Phys. Rev. Lett. **107**, 230402 (2011).
[14] D. Chen, M. White, C. Borries, and B. DeMarco, Phys. Rev. Lett. **106**, 235304 (2011).
[15] A. Das, J. Sabbatini and W. H. Zurek, Sci. Rep. **2**, 352 (2012).
[16] M. E. Dodd, P. C. Hendry, N. S. Lawson, P. V. E. McClintock, and C. D. H. Williams, Phys. Rev. Lett. **81**, 3703 (1998).
[17] G. Karra and R. J. Rivers, Phys. Rev. Lett. **81**, 3707 (1998); R. J. Rivers, *ibid.* **84**, 1248 (2000).
[18] L. M. A. Bettencourt, N. D. Antunes, and W. H. Zurek, Phys. Rev. D. **62**, 065005 (2000).
[19] P. Sikivie, Phys. Rev. Lett. **48**, 1156 (1982).
[20] C. N. Weiler, T. W. Neely, D. R. Scherer, A. S. Bradley, M. J. Davis, and B. P. Anderson, Nature **455**, 948 (2008).
[21] V. M. Kaurov and A. B. Kuklov, Phys. Rev. A **71**, 011601(R) (2005); *ibid.* **73**, 013627 (2006).
[22] J. Brand, T. J. Haigh, and U. Zülicke, Phys. Rev. A **80**, 011602(R) (2009).
[23] T. Fernholz, R. Gerritsma, P. Krüger, and R. J. C. Spreeuw, Phys. Rev. A **75**, 063406 (2007).
[24] A. Ramanathan, *et. al.*, Phys. Rev. Lett. **106**, 130401 (2011).
[25] L. Pitaevskii, S. Stringari, *Bose-Einstein Condensation* (Clarendon, Oxford, 2003).
[26] M. I. Qadir, H. Susanto, P. C. Matthews, J. Phys. B **45**, 035004 (2012).
[27] A. S. Bradley, M. J. Davis, C. W. Gardiner, Phys. Rev. A **77**, 033616 (2008).
[28] P. B. Blakie, A. S. Bradley, M. J. Davis, R. J. Ballagh, and C. W. Gardiner, Adv. Phys. **57**, 363-455 (2008).
[29] W. Zurek, Phys. Rep. **296**, 177 (1996).
[30] K. Henderson, C. Ryu, C. MacCormick and M. G. Boshier, New J. Phys. **11**, 043030 (2009).
[31] M. Pospelov, S. Pustelny, M. P. Ledbetter, D. F. Jackson Kimball, W. Gawlik, and D. Budker, Phys. Rev. Lett. **110**, 021803 (2013).